

SECTION 2: MODEL DESCRIPTION AND CAPABILITIES

2) Model Description and Capabilities

This two-part study addresses the concerns of desalination plant source discharge dilution and source water issues by utilizing a coupled set of numerical tidal and wave transport models to evaluate dilution and dispersion when the proposed desalination plant is functioning at its maximum production capacity of 50 mgd. The numerical model used to simulate tidal currents in the nearshore and shelf region of Newport/Huntington Beach is the finite element model **TIDE_FEM**. Wave-driven currents are computed from the shoaling wave field by a separate model, **OCEANRDS**. The dispersion and transport of concentrated seawater and storm water discharge by the wave and tidal currents is calculated by the finite element model known as **SEDXPORT**. The “wiring-diagram” showing the architecture for how these models were coupled together is shown in Figure 2.1.

The finite element research model, **TIDE_FEM**, (Jenkins and Wasyl, 1990; Inman and Jenkins, 1996) was employed to evaluate the tidal currents in a nearshore region extending between Seal Beach and Crystal Cove State Beach (Figure 1.3). **TIDE_FEM** was built from some well-studied and proven computational methods and numerical architecture that have done well in predicting shallow water tidal propagation in Massachusetts Bay (Connor and Wang, 1974) and along the coast of Rhode Island, (Wang, 1975), and have been reviewed in basic text books (Weiyan, 1992) and symposia on the subject, e.g., Gallagher (1981). The governing equations and a copy of the core portion of the **TIDE_FEM** FORTRAN code are found in Appendix B. **TIDE_FEM** employs a variant of the vertically integrated equations for shallow water tidal propagation after Connor and Wang (1975). These are based upon the Boussinesq

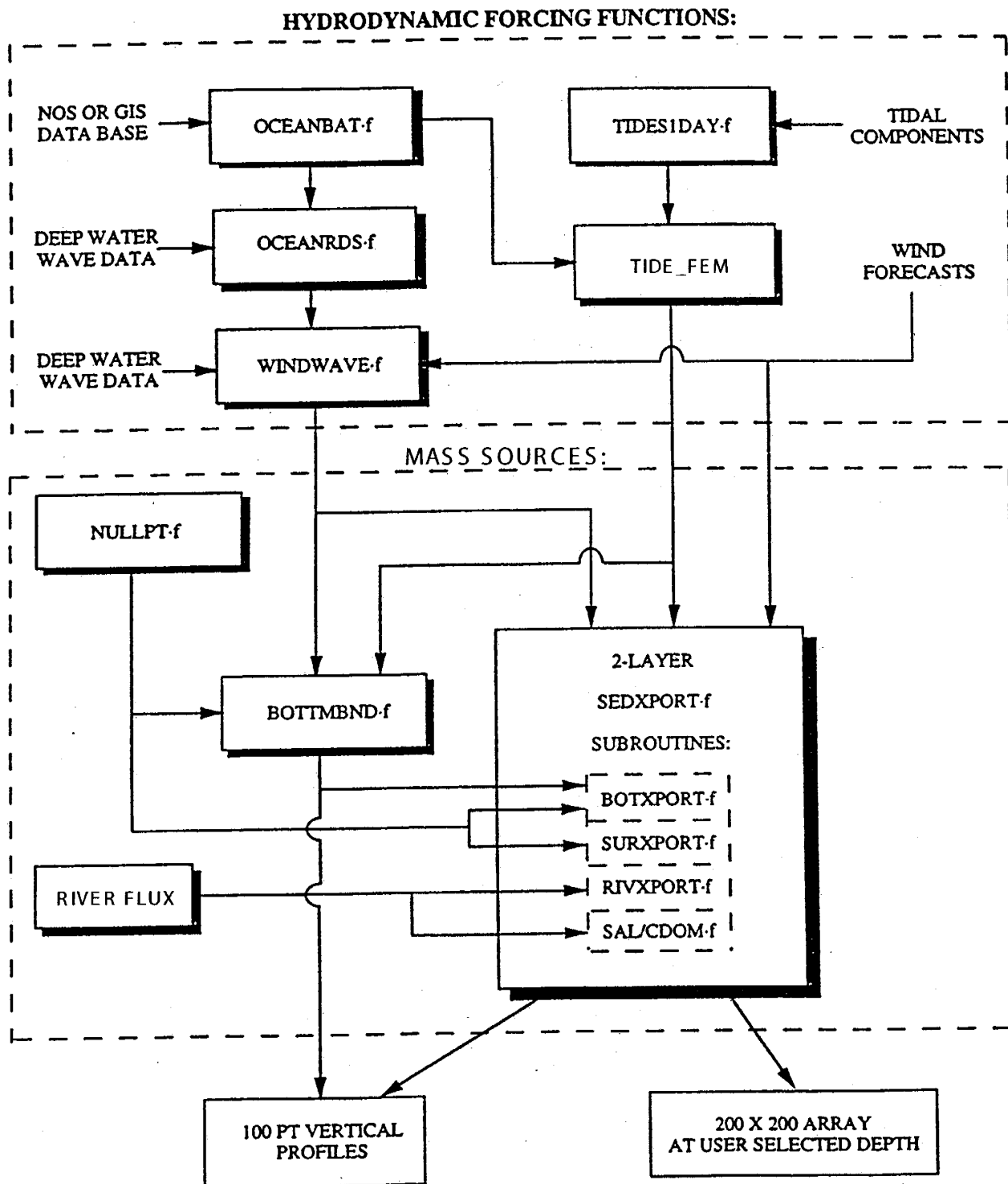


Figure 2.1. SEDXPORT architecture and computational sequence.

approximations with Chezy friction and Manning's roughness. The finite element discretization is based upon the commonly used **Galerkin weighted residual method** to specify integral functionals that are minimized in each finite element domain using a variational scheme, see Gallagher (1981). Time integration is based upon the simple **trapezoidal rule** (Gallagher, 1981). The computational architecture of **TIDE_FEM** is adapted from Wang (1975), whereby a transformation from a **global** coordinate system to a **natural** coordinate system based on the unit triangle is used to reduce the weighted residuals to a set of order-one ordinary differential equations with constant coefficients. These coefficients (**influence coefficients**) are posed in terms of a **shape function** derived from the natural coordinates of each nodal point in the computational grid. The resulting systems of equations are assembled and coded as banded matrices and subsequently solved by **Cholesky's method**, see Oden and Oliveira (1973) and Boas (1966). The hydrodynamic forcing used by **TIDE_FEM** is based upon inputs of the tidal constituents derived from Fourier decomposition of tide gage records. Tidal constituents are input into the module **TID_DAYS**, which resides in the hydrodynamic forcing function cluster (see Appendix C for a listing of **TID_DAYS** code). **TID_DAYS** computes the distribution of sea surface elevation variations at Huntington Beach and adjacent nearshore after compensating for phase shifts associated with travel time between the Los Angeles tide gage station (NOAA #941-0660) and Huntington Beach. Forcing for **TIDE_FEM** is applied by the distribution in sea surface elevation across the deep water boundary of the computational domain in Figure 1.3. Here the tidal currents reduce to the deep water solutions to Laplace's tidal equations (Lamb, 1932). The x-component (longitudinal) of the deep water tidal current is given by:

$$u_{x,\infty} = \frac{ig}{a} \left[\frac{2\Omega r \cot\theta (\xi - \bar{\xi}) + \omega \left(\frac{d\xi}{d\theta} - \frac{d\bar{\xi}}{d\theta} \right)}{\omega^2 - (2\Omega \cos\theta)^2} \right] \quad (1)$$

while the y-component (latitudinal) is:

$$u_{y,\infty} = \frac{g}{a} \left[\frac{r\omega \csc\theta (\xi - \bar{\xi}) \Omega \cos\theta \left(\frac{d\xi}{d\theta} - \frac{d\bar{\xi}}{d\theta} \right)}{\omega^2 - (2\Omega \cos\theta)^2} \right] \quad (2)$$

where θ is the co-latitude; $\bar{\xi}$ is the equilibrium tide; g is the acceleration of gravity; Ω is the angular speed of rotation of the earth, a is the mean radius of the earth; s is an integer; ω is the radian frequency of the potential tide as determined from the tidal constituents.

Wave driven currents were calculated from wave measurements by the CDIP arrays at Huntington Beach, San Clemente, Oceanside, CA, see CDIP (2004). These measurements were back refracted out to deep water to correct for island sheltering effects between the monitoring sites and AES Huntington Beach. The waves were then forward refracted onshore to give the variation in wave heights, wave lengths and directions throughout the nearshore around AES Huntington Beach. The numerical refraction-diffraction code used for both the back refraction from the San Clemente array out to deep water, and the forward refraction to the AES Huntington Beach site is **OCEANRDS** and may be found in Appendix D. This code calculates the simultaneous refraction and diffraction patterns of the swell and wind wave components propagating over bathymetry replicated by the

OCEANBAT-f code, (Figure 2.1). **OCEANBAT-f** generates the associated depth fields for the computational grid networks of both **TID_FEM** and **OCEANRDS** using packed bathymetry data files derived from the National Ocean Survey (NOS) depth soundings. The structured depth files written by **OCEANBAT-f** are then throughput to the module **OCEANRDS-f**, which performs a refraction-diffraction analysis from deep water wave statistics. **OCEANRDS-f** computes local wave heights, wave numbers, and directions for the swell component of a two-component, rectangular spectrum. These values are then throughput to **WINDWAVE-f**, which completes the refraction-diffraction analysis of the two-component spectrum including wind wave effects up to Nyquist frequencies.

The wave data computed throughout the domain of Figure 1.3 are throughput to a wave current algorithm in **SEDXPORT** which calculates the wave-driven longshore currents, $v(r)$. These currents were linearly superimposed on the tidal current. The wave-driven longshore velocity, $v(r)$, is determined from the longshore current theories of Longuet-Higgins (1970), according to:

$$\begin{aligned}\bar{v}(r) &= v_o \left(\frac{10}{49} \frac{r}{X_b} - \frac{5}{7} \ln \frac{r}{X_b} \right) \text{ if } 0 \leq r \leq X_b \\ &= v_o \frac{10}{49} \left(\frac{r}{X_b} \right)^{5/2} \text{ if } r > X_b\end{aligned}\quad (3)$$

$$v_o = \frac{5\pi}{8} \frac{0.41}{C_D} (gh_b)^{1/2} \beta \sin \alpha_b$$

where r is the shoreline-normal coordinate, X_b is the width of the surf zone, taken as $X_b \equiv 5/4 H_b \tan\beta$, H_b is the breaker height from the refraction solution, $\tan\beta$ is the beach slope, α_b is the breaker angle, h_b is the breaker depth, taken as $h_b = 5/4H_b$. C_D is the drag coefficient, and g is the acceleration of gravity. Inspection of (3) reveals that the longshore transport is strongest in the neighborhood of the breakpoint, $r = X_b$, where the longshore currents approach a maximum value of $v(r) = v_o$.

Once the tidal and wave driven currents are resolved by **TIDE_FEM** and **OCEANRDS** and **WINDWAVE**, the dilution and dispersion of flood water runoff and concentrated seawater discharge in those flows is computed by the stratified transport model **SEDXPORT** (Figure 2.1). The **SEDXPORT** code is a time stepped finite element model which solves the advection-diffusion equations over a fully configurable 3-dimensional grid. The vertical dimension is treated as a two-layer ocean, with a surface mixed layer and a bottom layer separated by a pycnocline interface. The code accepts any arbitrary density and velocity contrast between the mixed layer and bottom layer that satisfies the Richardson number stability criteria and composite Froude number condition of hydraulic state.

In both Section 6 of this study, the flood water runoff is represented as sources in the surface mixed layer while the concentrated seawater is represented by a point source either in the bottom layer or the mixed layer depending on the pycnocline cline depth of the particular model scenario. The AES infall is similarly treated as a sink. The source initializations for the Santa Ana River, Talbert Channel, OCSD outfall, AES outfall and infall are handled by a companion code called **MULTINODE** that couples the computational nodes of **TIDE_FEM** and **OCEANRDS** with **SEDXPORT**. The codes do not time split advection and

diffusion calculations, and will compute additional advective field effects arising from spatial gradients in eddy diffusivity, i.e., the so-called “gradient eddy diffusivity velocities” after Armi (1979). Eddy mass diffusivities are calculated from momentum diffusivities by means of a series of Peclet number corrections based upon TSS and TDS mass and upon the mixing source. Peclet number corrections for the surface and bottom boundary layers are derived from the work of Stommel (1949) with modifications after Nielsen (1979), Jensen and Carlson (1976), and Jenkins and Wasyl (1990). Peclet number correction for the wind-induced mixed layer diffusivities are calculated from algorithms developed by Martin and Meiburg (1994), while Peclet number corrections to the interfacial shear at the pycnocline are derived from Lazara and Lasheras (1992a;1992b). The momentum diffusivities to which these Peclet number corrections are applied are due to Thorade (1914), Schmidt (1917), Durst (1924), and Newman (1952) for the wind-induced mixed layer turbulence and to Stommel (1949) and List, et al. (1990) for the current-induced turbulence. The primitive equations for the **SEDXPORT** code may be found in Appendix E and in Appendix F for **MULTINODE**.

In its most recent version, **SEDXPORT** has been integrated into the Navy’s Coastal Water Clarity Model and the Littoral Remote Sensing Simulator (LRSS) (see Hammond, et al., 1995). The **SEDXPORT** code has been validated in mid-to-inner shelf waters (see Hammond, et al., 1995; Schoonmaker, et al., 1994). Validation of the **SEDXPORT** code was shown by three independent methods: 1) direct measurement of suspended particle transport and particle size distributions by means of a laser particle sizers; 2) measurements of water column optical properties; and, 3) comparison of computed stratified plume dispersion patterns with LANDSAT imagery. An example of the resolution of plumes by the **SEDXPORT**

model is shown in Figure 2.2 for the Santa Margarita River. In this figure the isocontours of suspended sediment concentrations computed by **SEDXPORT** (red lines) are overlaid on the LANDSAT image. The colored patchwork on the land delineate the primary and secondary drainage basins of streams discharging into the nearshore following the storm of 23 January 1993.

SEDXPORT has been built in a modular computational architecture (Figure 2.1). The modules are divided into two major clusters: 1) those which prescribe hydrodynamic forcing functions; and, 2) those which prescribe the mass sources acted upon by the hydrodynamic forcing to produce dispersion and transport. The cluster of modules for hydrodynamic forcing ultimately prescribes the velocities and diffusivities induced by wind, waves, and tidal flow for each depth increment at each node in the grid network.

The lower set of modules in Figure 2.1 compute the mixing and transport induced by the forcing functions acting on mass sources, including flood water runoff from the Santa Ana River and Talbert Channel and the concentrated seawater discharged from the RO process. The subroutine **BOTXPORT-f** in **SEDXPORT-f** solves for the mixing and advection of the negatively buoyant concentrated seawater in response to the wave and tidal flow using an rms vorticity-based time splitting scheme. The subroutine **RIVXPORT-f**, performs a similar computation on the positively buoyant flood water runoff from the Santa Ana River and Talbert Channel. Both **BOTXPORT** and **RIVXPORT** solve the eddy gradient form of the advection diffusion equation for the water column density field where u is the vector velocity from a linear combination of the wave

Comparison

Suspended Particulate--LANDSAT RGB Image

Modeled Concentration Contours (Log10)

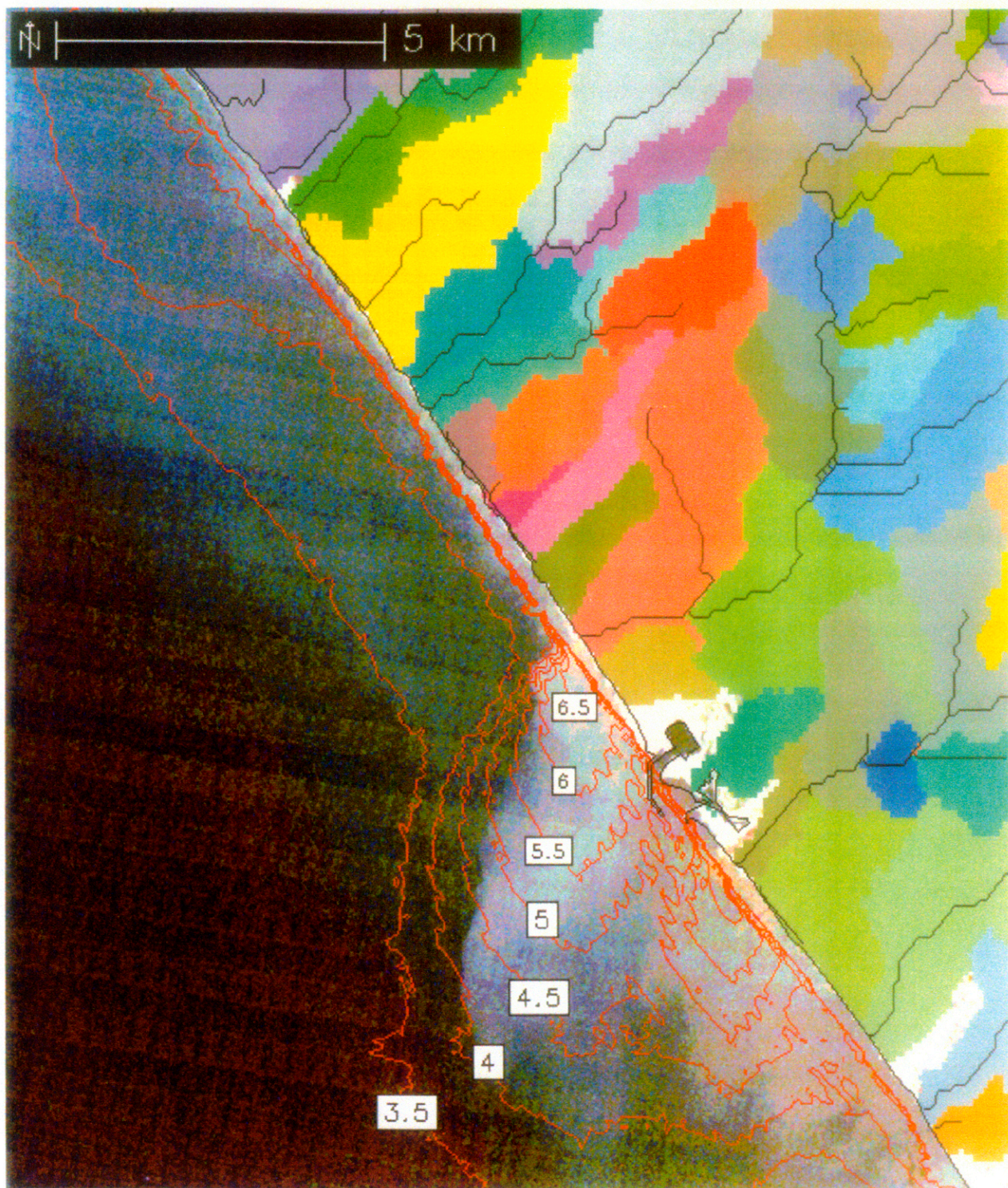


Figure 2.2. Comparisons of the SEDXPORT plume model with a LANDSAT image of the Santa Margarita River discharge on January 23, 1993. Modeled sediment concentration contours are expressed in base-10 log scale of particle number per ml. The color patchwork on the land denotes drainage basins of local streams.

$$\frac{\partial \rho}{\partial t} = (\mathbf{u} - \nabla \epsilon) \cdot \nabla \rho - \epsilon \nabla^2 \rho \quad (4)$$

and tidal currents, ϵ is the mass diffusivity and ρ is the water mass density. The water mass density is a function of temperature, T , and salinity, S , according to the equation of state expressed in terms of the specific volume, $\alpha = 1/\rho$, or:

$$\frac{d\alpha}{\alpha} = \frac{1}{\alpha} \frac{\partial \alpha}{\partial T} dT + \frac{1}{\alpha} \frac{\partial \alpha}{\partial S} dS \quad (5)$$

The factor $\partial\alpha/\partial T$, which multiplies the differential temperature changes, is known as the coefficient of thermal expansion and is typically 2×10^{-4} per $^{\circ}\text{C}$ for seawater; the factor $\partial\alpha/\partial S$ multiplying the differential salinity changes, is the coefficient of saline contraction and is typically 8×10^{-4} per part per thousand (ppt) where 1.0 ppt = 1.0 g/L of total dissolved solids (TDS). For a standard seawater, the specific volume has a value $\alpha = 0.97264$. If the percent change in specific volume by equation (5) is less than zero, then the new water mass is heavier than standard seawater, and lighter if the percent change is greater than zero. Solutions to the density field calculated from equation (1) by **SEDXPORT** are used to calculate the field salinity, $S_{(x, y, z)}$, from equation (5) for an assumed T for the ambient ocean and river water and ΔT for plant thermal effluent. The salinity field in turn can be used to solve for the spacial varying dilution factor, $D_{(x, y, z)}$ according to:

* Fresh Water Runoff Dilution:

$$D_{(x,y,z)} = \frac{S_o}{S_o - S_{(x,y,z)}} \quad (6)$$

** Concentrated Seawater Dilution:

$$D_{(x,y,z)} = \frac{S_b - S_o}{S_{(x,y,z)} - S_o} \quad (7)$$

where S_o is the ambient seawater salinity in ppt, S_b is the end-of-the-pipe salinity of concentrated seawater and $S_{(x,y,z)}$ is the local salinity from the model solution in ppt. In equation (6) the total dissolved solids of the fresh water runoff is assumed to be 0.0 ppt. Model solutions will find a significant variation in the salinity with water depth, z . Therefore we introduced a depth averaged dilution factor, \bar{D} :

$$\bar{D}_{(x,y,z)} = \frac{1}{H_{(x,y)}} \int_0^H D_{(x,y,z)} dz \quad (8)$$

where $H = H_{(x,y)} = h + \eta$ is the local water depth, h is the local water depth below mean sea level and η is the tidal amplitude.

The diffusivity, ϵ , in equation (4) controls the strength of mixing and dilution of the concentrated seawater and flood water constituents, and varies with position

in the water column relative to the pycnocline interface. Vertical mixing includes two mixing mechanisms at depths above and below the pycnocline: 1) fossil turbulence from the bottom boundary layer, and 2) wind mixing in the surface mixed layer. The pycnocline depth is treated as a zone of hindered mixing and varies in response to the wind speed and duration. Below the pycnocline, only turbulence from the bottom wave/current boundary layer contributes to the local diffusivity. Nearshore, breaking wave activity also contributes to mixing. The surf zone is treated as a line source of turbulent kinetic energy by the subroutine **SURXPORT-f**. This subroutine calculates seaward mixing from fossil surf zone turbulence, and seaward advection from rip currents embedded in the line source. Both the eddy diffusivity of the line source and the strength and position of the embedded rip currents are computed from the shoaling wave parameters evaluated at the breakpoint, as throughput of **OCEANRDS-f**.